Synthesis, crystal structural, and spectral characterisation of dabigatran etexilate tetrahydrate

Zhi-Qiang Cai[a], Xu Hou[a], Du-Lin Kong[b]*, Ling Hou[a] and Zhi-Quan Hu[a]

[a]*School of Petrochemical Engineering, Shenyang University of Technology, Liaoyang 111003, Liaoning Province, P.R. China*
[b]*School of Pharmaceutical Sciences, Hainan Medical University, Haikou 571199, Hainan Province, P.R. China*

Dabigatran etexilate tetrahydrate, $C_{34}H_{49}N_7O_9$, has been crystallised at ambient conditions. The colourless crystal was investigated using X-ray crystallography with single crystals and powder techniques, and was characterised by thermogravimetric-differential thermal analysis (TG-DTA) and infrared spectroscopy (IR). The compound was shown to be a tetrahydrate. A dabigatran etexilate molecule and four water molecules form a large ring structure, and intra-molecular hydrogen bonds contribute to the formation of a stable molecule in the unit cell.

Keywords: dabigatran etexilate, thrombin inhibitor, tetrahydrate, crystal structure, thermal analysis

Since the last decade, more attention has been focused on the investigation of pharmaceutical behaviours of hydrates. One third of active pharmaceutical ingredients (APIs) are capable of forming hydrates during pharmaceutical processing, which led to a potential altered performance of the drug.[1–3] The improved solubility of APIs in the form of organic crystal hydrates make them potent novel drugs with increased therapeutic effectiveness and bioavailability.[4–9] Variations due to hydration induce dosage variations including drug bioavailability, solubility, and stability. Thus, solid form screening is crucial in the early stages of drug development and more importantly during pharmaceutical processing where factors such as pressure, temperature, and humidity can alter the crystalline form of the API.

Dabigatran etexilate mesylate, ethyl 3-[({2-[(4-{*N*'-[(hexyloxy)carbonyl]carbamimidoyl}anilino)methyl]-1-methyl-1*H*-benzimidazol-5-yl}carbonyl)(pyridin-2-yl)amino]propanoate methanesulfonate (Fig. 1), is a potent, orally active, direct thrombin inhibitor which was developed by Boehringer Ingelheim. Dabigatran etexilate mesylate was approved by the EMEA in 2008 (prevention of venous thromboembolism after total hip replacement) and the FDA in 2010 (prevention of atrial fibrillation).[10–22]

Dabigatran etexilate has poor water-solubility (pH > 4, almost insoluble in water) and commercial dabigatran etexilate is in the form of its mesylate with solubility of 1.8 mg mL^{-1} at 25 °C.[23] In this study, the tetrahydrate of dabigatran etexilate is characterised, showing better solubility and stability than the anhydrous form, so it is expected to become a commercial drug after further optimisation. The crystallisation of the tetrahydrate from common solvents is a major challenge. We were able to crystallise dabigatran etexilate as a hydrate, with the ratio 1:4 (dabigatran etexilate:water), and single crystal X-ray structures of the hydrated form was determined for the first time offering an insight into the solvation behaviour of this important drug.[24] Unfortunately, after trying numerous ways, we have not developed a single-crystal form of the anhydrous form. Additionally, both the anhydrous form and tetrahydrate forms were characterised by powder X-ray diffraction (PXRD), thermogravimetric-differential thermal analysis (TG-DTA) and infrared spectroscopy (IR). Solubility measurements on the tetrahydrate form and anhydrate phase in water show that the hydrate has a major solubility advantage over the anhydrous form.

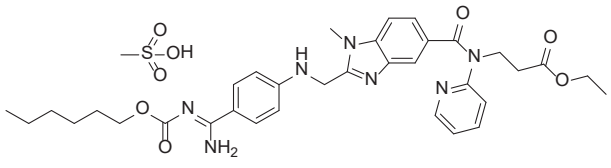

Fig. 1 Molecular structure of dabigatran etexilate.

Results and discussion

Powder X-ray diffraction of dabigatran etexilate

Microcrystalline samples of the anhydrous form and the tetrahydrate of dabigatran etexilate phases were characterised by PXRD to ensure phase identity (Fig. 2).

Dabigatran etexilate tetrahydrate has a relatively bigger reflection and sharp peak than the anhydrous form, which is observed at 21.70 2θ. The other characteristic peaks of tetrahydrate observed at 4.54, 19.56 and 24.64 2θ compared to the anhydrous form which has characteristic peaks at 8.87, 15.91, 20.34 and 25.39 2θ. Both powder diffraction patterns are very distinctive. It confirms that the product is an individual compound without any impurities including dabigatran etexilate and water in the amounts detectable by this technique.

Single crystal structure of dabigatran etexilate tetrahydrate

The dabigatran etexilate tetrahydrate was considered as a hydrate of dabigatran etexilate (Fig. 3). The composition ratio equalled 1:4 (dabigatran etexilate:water). The compound crystallised with a triclinic lattice with a = 9.1140(13) Å, b = 10.9700(14) Å, c = 18.3830(17) Å, α = 88.510(10) °, β = 85.455(9) °, γ = 83.034(12) °, Z = 2, V = 1818.4(4) $Å^3$, S.G. P-1. The crystal structure determination demonstrates the importance of inter- and intra-molecular interactions in the crystal formation. A dabigatran etexilate molecule and four water molecules form a large ring structure, and intra-molecular hydrogen bonds contribute to the formation of a stable molecule in the unit cell. These data were further confirmed by X-ray single crystal investigation (Table 1). In the dabigatran etexilate tetrahydrate, the benzene and pyridine rings form dihedral angles of 5.4(1) and 43.8(1) °, respectively, with the benzimidazole mean plane. The terminal butyl group is disordered over two conformations in a ratio 0.756(1):0.244(1). The crystalline water molecules are involved in formation of

* Correspondent. E-mail: kahongzqc@163.com

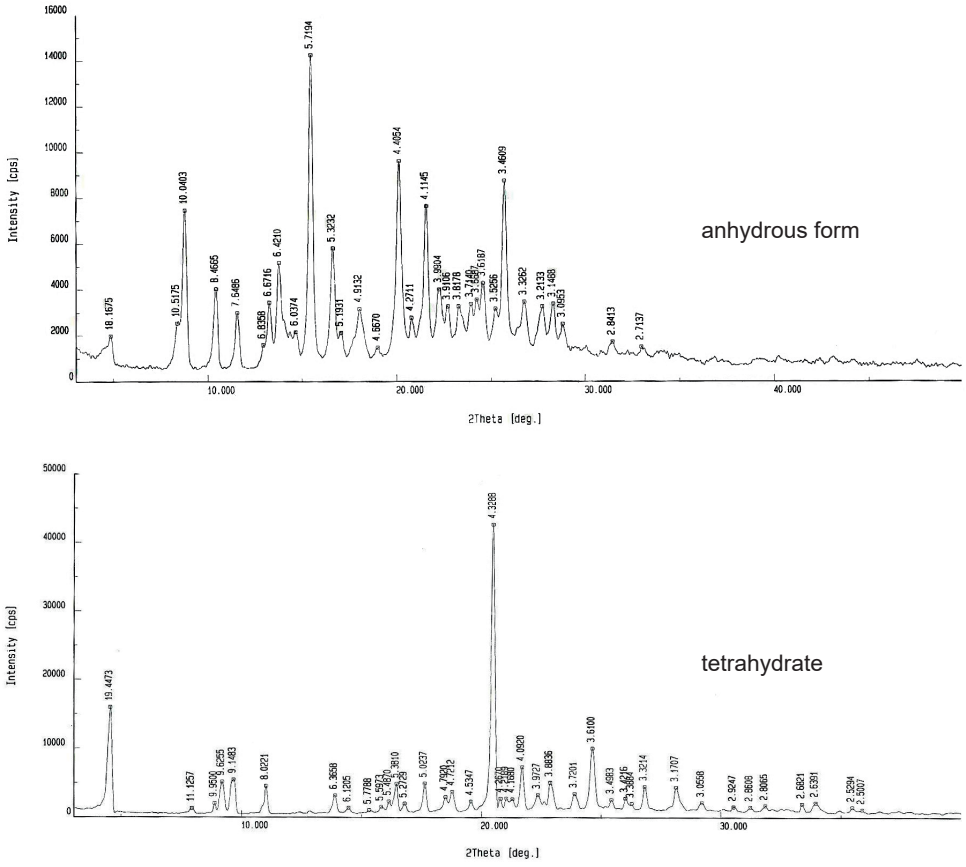

Fig. 2 PXRD pattern of anhydrous and tetrahydrate phases of dabigatran etexilate.

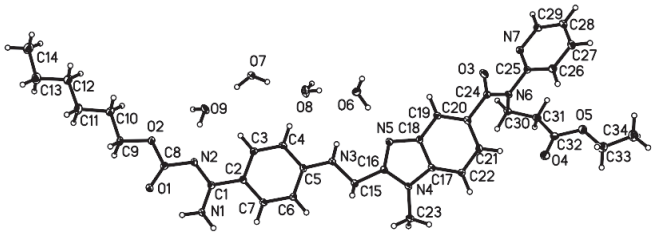

Fig. 3 ORTEP diagram of dabigatran etexilate tetrahydrate. Thermal ellipsoids are drawn at 30% probability.

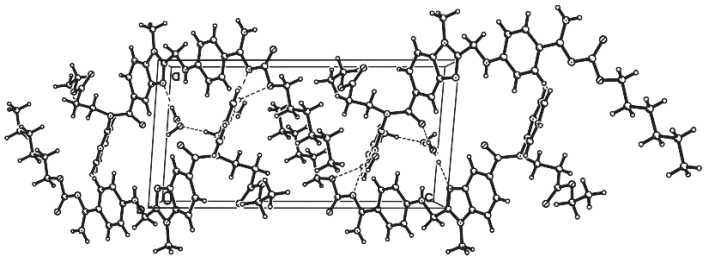

Fig. 4 A packing diagram for dabigatran etexilate tetrahydrate.

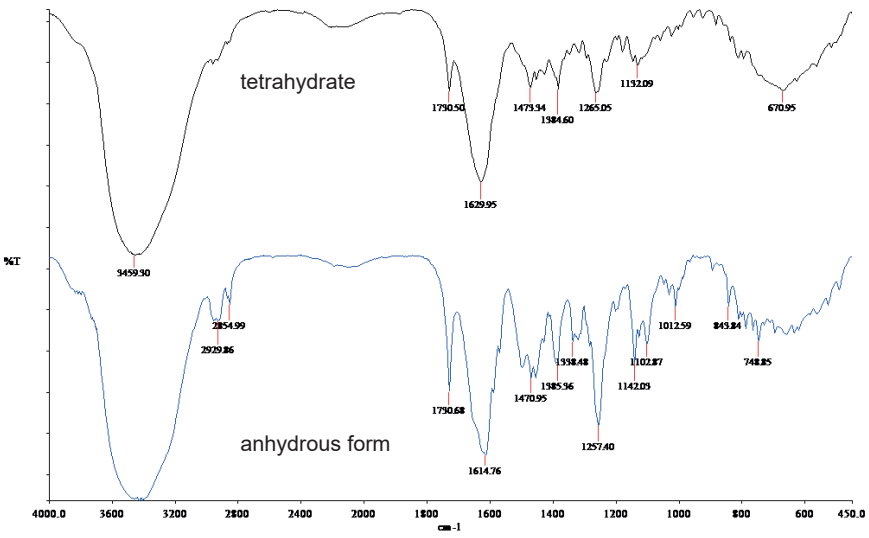

Fig. 5 IR spectrum for anhydrate and tetrahydrate phases of dabigatran etexilate.

Table 1 Summary of crystal data for dabigatran etexilate tetrahydrate

Empirical formula	$C_{34}H_{49}N_7O_9$
Formula weight	699.8
Temperature	293 K
Wavelength	0.71075 A
Crystal system, space group	Triclinic, P-1
Unit cell dimensions	a = 9.1140(13) Å
	b = 10.9700(14) Å
	c = 18.3830(17) Å
	α = 88.510(10) °
	β = 85.455(9) °
	γ = 83.034(12) °
Volume	1818.4(4) $Å^3$
Z, Calculated density	2, 1.278 mg $m3^{-1}$
Absorption coefficient	0.094 mm^{-1}
F (000)	748
Crystal size	0.22 × 0.20 × 0.18 mm
Theta range for data collection	1.87–27.89 °
Limiting indices	−11 ≤ h ≤ 11,
	−14 ≤ k ≤ 14,
	−24 ≤ l ≤ 24
Reflections collected/unique	23569/8627[R(int) = 0.0356]
Completeness to theta = 27.89	99.40%
Absorption correction	Semi-empirical
	from equivalents
Max. and min. transmission	0.9833 and 0.9797
Refinement method	Full-matrix least-squares on F^2
Data / restraints / parameters	8627 / 40 / 513
Goodness-of-fit on F^2	0.962
Final R indices [I > 2sigma(I)]	*R*1 = 0.0386, wR2 = 0.0970
R indices (all data)	*R*1 = 0.0567, wR2 = 0.1025
Extinction coefficient	0.0080(11)
Largest diff. peak and hole	0.415 and −0.367 $eÅ^{-3}$

O–H…O, O–H…N and N–H…O hydrogen bonds (Table 2), which link all moieties into layers parallel to the *ab* plane (Fig. 4). Unfortunately, after trying numerous ways, we have not developed a single-crystal of the anhydrous form.

Spectral studies of dabigatran etexilate

The IR spectrum of the compound, (dabigatran etexilate tetrahydrate), is characterised by a very strong carbonyl stretching peak at 1730 cm^{-1} (Fig. 5). It is assigned to the C=O stretch which superimposes with the C=O stretch of the ester groups or acyl groups. A broad band centred at 3459 cm^{-1} is assigned to the stretching of the hydrogen bonded NH of the NH_2 group.

The ^{1}H NMR spectra of the compound, dabigatran etexilate tetrahydrate in $CDCl_3$ (Fig. 6) display one signal at 3.66 ppm (3H), corresponding to the protons of NCH_3. The aromatic protons give a group of multisignals at 6.61–8.39 ppm (10H). The ammonium protons NH_2 which are involved in extensive hydrogen bonding are not observed in $CDCl_3$. The proton of the H_2O group is detected as a broad band at 1.39–2.14 ppm (8H), where an anhydrous form is not observed.

The mass spectrum of the compound shows a well-defined parent peak at *m/z* = 628 $[M + H]^+$ and 650 $[M + Na]^+$. The peak of the H_2O group is not detected in the mass spectrum of the dabigatran etexilate tetrahydrate.

Table 2 Hydrogen bond interactions in dabigatran etexilate tetrahydrate [Å and °]

D–H...A	d(D–H)/Å	d(H..A)/Å	d(D..A)/Å	< DHA/°
N(1)–H(1)...O(7)#1	0.896(17)	1.980(18)	2.8468(16)	162.5(15)
N(1)–H(2)...O(1)	0.902(15)	1.931(16)	2.6281(16)	132.7(13)
N(3)–H(5)...O(6)	0.826(15)	2.644(16)	3.4533(17)	166.8(15)
O(6)–H(8)...N(5)	0.912(19)	1.88(2)	2.7938(16)	176.3(16)
O(6)–H(16)...O(3)#2	0.84(2)	2.00(2)	2.8373(15)	172.1(18)
O(7)–H(17)...O(8)	0.861(19)	1.954(19)	2.8061(16)	170.2(18)
O(7)–H(18)...O(9)	0.881(18)	1.871(19)	2.7513(15)	176.5(17)
O(9)–H(20)...N(2)	0.93(2)	2.00(2)	2.9226(16)	168.8(19)
O(9)–H(20)...O(2)	0.93(2)	2.43(2)	3.1126(14)	129.6(16)
O(9)–H(24)...N(7)#3	0.844(19)	2.050(19)	2.8918(16)	175.5(18)
O(8)–H(25)...O(6)	0.84(2)	2.04(2)	2.8689(17)	171(2)
O(8)–H(32)...O(6)#3	0.94(2)	1.89(2)	2.8291(17)	175.3(17)

Symmetry transformations used to generate equivalent atoms:
#1 x – 1,y,z; #2 –x + 1, –y + 2,–z + 2; #3 –x + 1,–y + 1,–z + 2.

Thermal study of dabigatran etexilate

In order to examine the thermal stability of the new compound, the thermogravimetric analysis of dabigatran etexilate tetrahydrate and anhydrate dabigatran etexilate were carried out in the temperature range 25–300 °C in nitrogen atmosphere (Fig. 7).

TG was performed on tetrahydrate and anhydrate phase from 25 °C to 300 °C. The mass change of tetrahydrate and anhydrous phase is 45.8% and 39.1%, respectively. The tetrahydrate and anhydrate phases were analysed by DTA. It is interesting that anhydrate displays two endothermic events upon heating. The first endothermic transition is observed 81 °C, whereas the second event is centred at 129 °C in accordance with melting. DTA analysis of the tetrahydrate reveals a single endothermic effect centred at 86 °C indicating the melting point; no other phase transformations were observed during heating. This one step weight loss process confirms that the title compound is a crystalline hydrate, with a remarkably stable hydrogen bonded framework, as evidenced by single crystal X-ray structure.

Solubility measurement

Since solubility and drug dissolution are related to drug absorption, some studies have focused on the effect of tetrahydrate/anhydrous form on solubility. Dabigatran etexilate is a poorly water-soluble drug (pH > 4, almost insoluble in water) and commercial dabigatran etexilate is the form of its mesylate with solubility of 1.8 mg mL^{-1} at 25 °C. Solubility of dabigatran etexilate tetrahydrate was analysed in water at 25 ± 2 °C, which has better solubility in water (2.4 mg mL^{-1}) than the dabigatran etexilate mesylate. As the tetrahydrate form can produce much more concentrated solutions of dabigatran etexilate over sustained times, it may be a better candidate for formulation of this important drug than the currently used dabigatran etexilate mesylate.

Bioavailability

From these experiments oral bioavailabilities of dabigatran etexilate tetrahydrate and anhydrous dabigatran etexilate were calculated (Table 3). Oral bioavailabilities of dabigatran etexilate tetrahydrate in rats are higher than 20% at 10 mg kg^{-1}. At 10 mg kg^{-1} the oral bioavailability of dabigatran etexilate tetrahydrate (25.5%) was much higher than that of dabigatran etexilate (4.8%), and the value found for dabigatran etexilate

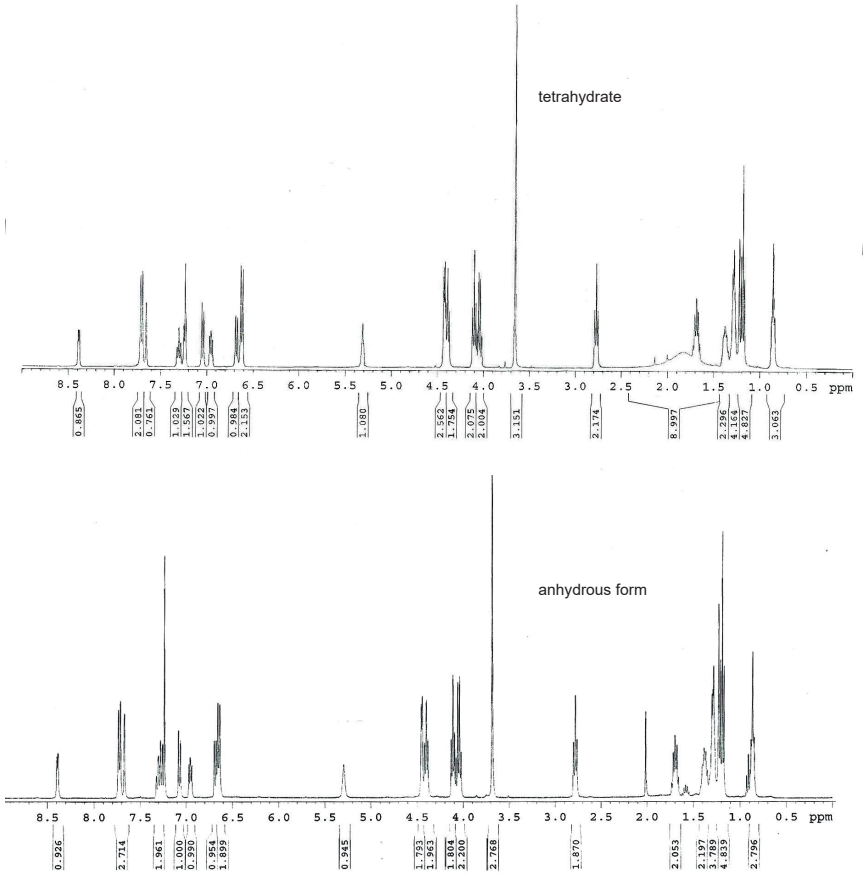

Fig. 6 ^{1}H NMR spectrum for anhydrate and tetrahydrate phases of dabigatran etexilate.

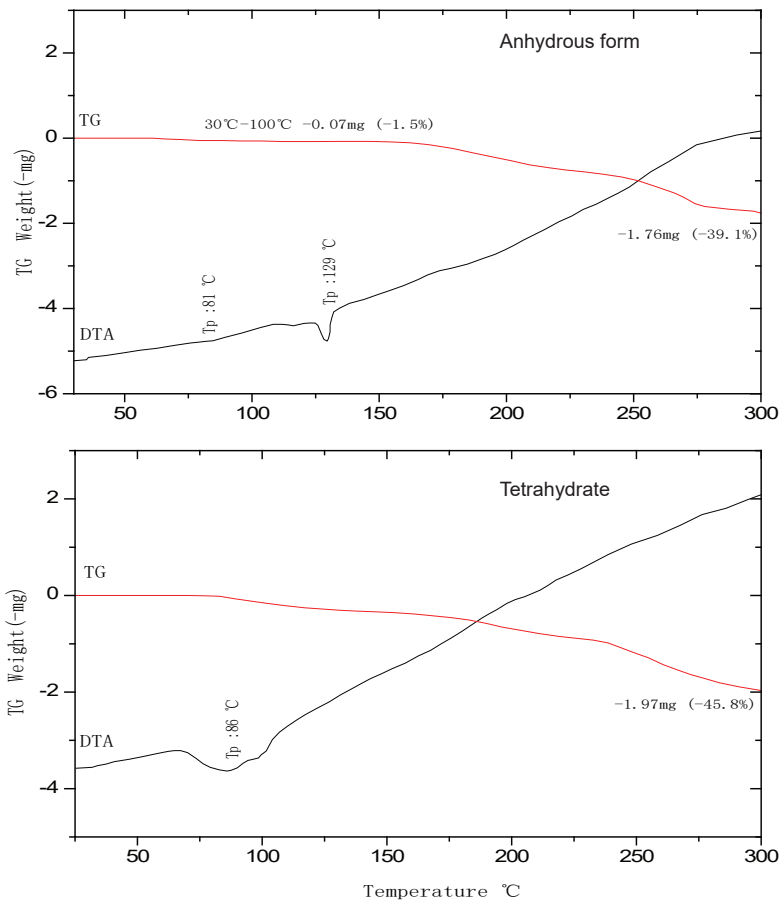

Fig. 7 TG and DTA curves of anhydrate and tetra hydrate phases of dabigatran etexilate.

Table 3 Oral bioavailabilities of dabigatran etexilate tetrahydrate and anhydrous dabigatran etexilate in the rat (n= 6)

dabigatran etexilate tetrahydrate/ dabigatran (dose p.o./i.v.)		dabigatran etexilate/dabigatran (dose p.o./i.v.)	
10/1 mg kg^{-1}	25.5 ± 2.8%	10/1 mg kg^{-1}	4.8 ± 0.2%

tetrahydrate was five-fold higher than that of dabigatran etexilate. Our results demonstrate that tetrahydrate dabigatran etexilate is highly absorbable by the rat and confirm its favourable physicochemical properties for oral absorption.

Conclusion

In conclusion, a novel pharmaceutical dabigatran etexilate tetrahydrate was prepared. X-ray single crystal and powder diffraction, TG-DTA and IR spectroscopy were used for the compound characterisation. The results obtained from these techniques are consistent. The product obtained by crystallisation from the acetone and water solution was the single phase substance. The thermal and X-ray phase analysis showed that the reaction between the precursors was completed and the obtained crystalline tetrahydrate was of high purity. Dabigatran etexilate tetrahydrate obtained in our present study is stable and has major solubility advantages which showed good bioavailability that may motivate using this form over the commercial anhydrate modification in future formulations of this important oral antithrombosis agent.

Experimental

All the chemicals were used as received without any further purification. Melting point was taken on a Beijing Taike X-4 microscopy melting point apparatus and were uncorrected. ^{1}H NMR spectra were recorded on a Bruker AV-400 MHz instrument using TMS as the internal standard. All chemical shifts were reported in ppm. IR spectra were recorded as KBr pellets on a PerkinElmer Spectrum One FTIR spectrometer. Dabigatran etexilate $C_{34}H_{41}N_7O_5$, with ≥ 98.0% of purity was synthesised from our laboratory.[23–27]

Synthesis of dabigatran etexilate tetrahydrate: 3-({2-[(4-Carbamimidoyl-phenylamino)methyl]-1-methyl-1*H*-benzoimidazole-5-carbonyl}pyridin-2-yl-amino)propionic acid ethyl ester (1.0 g, 1.86 mmol) was dissolved in 50 mL of THF and 10 mL of water. Potassium carbonate (0.83 g, 6.0 mmol) was added, and the mixture was stirred at room temperature for 15 min. Then, hexyl chloroformate (0.31 g, 1.86 mmol) was added and stirring was continued for another hour. The organic phase was separated, dried over anhydrous sodium sulfate, and concentrated *in vacuo*. The residue was left in 10 mL mixtured solution (acetone:water = 1:1) at room temperature for slow evaporation in air. Colourless needle crystals of the target compound formed after approximately three days, yield 59.7%, m.p. 127~129 °C, IR (KBr), σ/cm^{-1}: 3459.30, 1730.50, 1629.95, 1473.34, 1384.60, 1265.05, 1132.09, 670.95. ESI-MS(*m/z*) : 628 $[M + H]^+$, 650 $[M + Na]^+$. ^{1}H NMR ($CDCl_3$, 400 MHz): δ 0.84 (t, 3H), 1.17 (t, 3H), 1.19 (m, 6H), 1.39–2.14 (bs, 8H), 1.65 (m, 2H), 2.76 (t, 2H), 3.66 (s, 3H), 4.02 (m, 4H), 4.37 (t, 2H), 4.41 (d, 2H), 6.61 (d, 2H), 6.67 (d, 1H), 6.96 (t, 1H), 7.04 (m, 2H), 7.23 (d, 1H), 7.28 (d, 1H), 7.66 (s, 1H), 7.70 (d, 2H), 8.39 (dd, 1H).

Physical measurements

X-ray powder diffraction data were obtained using the diffractometer equipped with a graphite monochromated Mo Kα radiation (λ = 0.71073 Å) at 293 K. The structure was solved by direct methods using SHELXS-97 implemented in the WinGX software system and refined by full-matrix least-squares procedure using SHELXL-97.[28,29] The sample was grinded in an agate mortar and prepared in a standard cuvette by direct loading. For single crystal investigation a crystal of 0.22 × 0.20 × 0.18 mm dimensions was chosen. The absorption corrections were applied using the RAPID-AUTO *via* the multi-scan method.[30] The structure was solved using the direct methods SHELXS and refined in anisotropic approach for non-hydrogen atoms using the SHELXTL program. The hydrogen atoms were located by the difference electron density maps. All the hydrogen atoms connected with the carbon atoms were refined in a constrained mode, all the other were refined as independent ones. The experimental data and the refinement conditions are listed in Table 1. The crystallographic data are deposited in Cambridge Crystallographic Data Centre (CCDC: 914353).

The IR spectra were recorded on a PerkinElmer Spectrum One FTIR spectrometer in the range of 450–4000 cm^{-1}. The samples were prepared in the form of tablets 3 mm thick. Dry KBr was used as the filling material. Thermal analysis was carried out using PTC-10A TG-DTA (Japan) in the temperature range 25–300 °C, in air atmosphere. The substance (5 mg) was loaded into a platinum crucible. The heating rate was 10 °C min^{-1}.

Bioavailability measurements

The compounds were administered intravenously (IV) and orally (PO) to male Sprague-Dawley rats (n = 6) to evaluate the bioavailability of the dabigatran etexilate tetrahydrate and anhydrous dabigatran etexilate. Plasma concentrations of dabigatran etexilate tetrahydrate and anhydrous dabigatran etexilate were determined by LC/MS/MS. The plasma sample was processed using acetonitrile precipitation, then the supernatant was injected onto the LC column. The limit of quantitation of the assay was 0.1–5 nM. Pharmacokinetic data were analysed by WinNonlin, using compartmental and non-compartmental analysis for IV and PO data, respectively. Bioavailability (F) in rats were evaluated in jugular vein (JV) cannulated animals. The plasma concentrations of the compounds in the jugular vein were quantified and used to calculate the area-under-the-curve (AUC). Bioavailability were calculated from dose-normalised AUC values as follows: $F = AUC_{PO,JV}/AUC_{IV,JV}$.

This work was supported by the Scientific Research Foundation of the Education Department of Liaoning Province (L2015383) and the Doctoral Start-Up Fund of Shenyang University of Technology (No. 521422).

Received 18 February 2016; accepted 3 June 2016
Paper 1603927 doi: 10.3184/174751916X14664340623037
Published online: 22 July 2016

References

1 I. Jeffrey, M.D. Weitz and J. Hirsh, *Chest*., 2001, **119**, 95S.
2 K. Wåhlander, M. Eriksson-Lepkowska, L. Frison, G. Fager and U.G. Eriksson, *Clin. Pharmacokine*., 2003, **42**, 755.
3 J.A. Wilson, B. Goralski, S.D. Soroka, M. Morrison, P. Mossop, L. Sleno, Y. Wang and D.R. Anderson, *J. Clin. Pharmacol*., 2014, **54**, 901.
4 P.P. Dobesh and J. Fanikos, *Drugs*, 2014, **74**, 2015.
5 O.O. Beliavskaia and T.V. Vavilova, *Angiol. Sosud. Khir*., 2014, **20**, 37.
6 J. Hirsh and V. Fuster. *Circulation*., 1994, **89**, 1449.
7 B.I. Eriksson, P. Wille-Jørgensen, P. Kälebo, P. Mouret, N. Rosencher, P. Bösch, M. Baur, S. Ekman, D. Bach, S. Lindbratt and P. Close, *N. Engl. J. Med*., 1997, **337**, 1329.
8 M.R. Wiley and M.J. Fisher, *Expert. Opin. Ther. Pat*., 1997, **7**, 1265.
9 J. Das and S.D. Kimball, *Bioorg. Med. Chem*., 1995, **3**, 999.
10 Food and Drug Administration, *FDA Drug safety communication: update on the risk for serious bleeding events with the anticoagulant Pradaxa*, 2012; http://www.fda.gov/Drugs/DrugSafety/ucm326580.htm. [accessed November 2012].
11 S. Barco, M. Coppens, E.J. van den Dool, D. van de Kerkhof, A.K. Stroobants and S. Middeldorp, *Thromb. Haemost*., 2014, **112**, 836.
12 S.L. Greig and K. McKeage, *Drugs*, 2014, **74**, 1785.
13 H. Calkins, E.P. Gerstenfeld, R. Schilling, A. Verma and S. Willems, *Am. J. Cardiol*., 2015, **115**, 154.
14 J. Li, J. Fang, F. Zhong, W. Li, Y. Tang, Y. Xu, S. Mao and G. Fan, *J. Chromatogr. B. Analyt. Technol. Biomed. Life. Sci*., 2014, **973**, 110.
15 W. Wienen, J.M. Stassen, H. Priepke, U.J. Ries and N. Hauel, *Thromb. Haemost*., 2007, **98**, 155.
16 S. Blech, T. Ebner, E. Ludwig-Schwellinger, J. Stangier and W. Roth, *Drug Metab. Dispos.,* 2008, **36**, 386.
17 K. Huber, S.J. Connolly, A. Kher, F. Christory, G.A. Dan, R. Hatala, R.G. Kiss, B. Meier, B. Merkely, B. Pieske, T. Potpara, J. Stępińska, N.V. Klun, D. Vinereanu and P. Widimský, *Int. J. Clin. Pract*., 2013, **67**, 516.

18 T. Davidson, M. Husberg, M. Janzon, J. Oldgren and L.A. Levin, *Eur. Heart. J*., 2013, **34**, 177.

19 S. Blech, T. Ebner, E. Ludwig-Schwellinger, J. Stangier and W. Roth, *Drug. Metab. Dispos*., 2008, **36**, 386.

20 J.W. Eikelboom, D.J. Quinlan, S.J. Connolly, R.G. Hart and S. Yusuf, *J. Thromb. Haemost*., 2012, **10**, 966.

21 R.G. Hart, H.C. Diener, S. Yang, S.J. Connolly, L.P.A. Wallentin, Reilly, M.D. Ezekowitz and S. Yusuf, *Stroke*, 2012, **43**, 1511.

22 M. Gliem, D. Hermsen, N. van Rooijen, H.P. Hartung and S. Jander, *Stroke*, 2012, **43**, 3352.

23 N.H. Hauel, H. Nar, H. Priepke, U. Ries, J.M. Stassen and W. Wienen, *J. Med. Chem*., 2002, **45**, 1757.

24 H.Q. Liu, W.G. Zhang, Z.Q. Cai, W.R. Xu and X.P. Shen, *Acta. Cryst. E,* 2012, **E 68**, 3385.

25 J. Jirman, J. Richter and P. Lustig. Pat. Appl. WO 2009/111997, 17 September 2009.

26 P. Lustig and J. Jirman. Pat. Appl. WO 2010/045900, 29 April 2010.

27 D.J. Brian, G.A. David, A.C. Tracey, E. Brian and E.S. Tsarina, *Synth. Comm*., 1996, **26**, 4351.

28 G.M. Sheldrick, *SHELXTS-97 and SHELXTL-97.* University of Göttingen, Germany, 1997.

29 G.M. Sheldrick, *SHELXTL, Version 5.1.* Bruker AXS, Inc., Madison, Wisconcin, USA, 1997.

30 Rigaku/MSC, *CrystalClear.* Rigaku/MSC, TheWoodlands, Texas, USA, 2005.